# Wall effects in critical systems: Scaling in Ising model strips

Helen Au-Yang and Michael E. Fisher
*Baker Laboratory, Cornell University, Ithaca, New York 14853*
(Received 30 October 1979)

A scaling theory and a related conjecture presented recently by de Gennes and Fisher to predict the effects of walls inserted in two near-critical binary fluid mixtures, are checked theoretically by exact analytic calculations for $n \times \infty$, two-dimensional Ising model strips with a surface field, $h_1$, imposed on the first layer; exact calculations with a second surface field, $h_n$, imposed on the $n$th layer are also reported. It is verified, in particular, that the effects on properties observed close to one wall of a second wall at distance $D$ decay, at the critical point, as $1/D^d$, where $d$ is the spatial dimensionality. In addition to the scaling limits, the leading corrections are calculated explicitly and presented graphically.

## I. INTRODUCTION

Recently, de Gennes and Fisher[1] have discussed theoretically phenomena associated with the presence of a plane wall or pair of parallel walls in a binary fluid mixture $AB$ near its demixing or critical point. Various experiments were suggested, and predictions for their outcome were made on the basis of a scaling analysis. The composition, $\Phi(z)$, at distance $z$ from a plane wall, measured, say, by the local mole fraction of species $A$, will deviate from the overall or mean composition, $\bar{\Phi}$, since the wall will be more attractive to one species than to the other. This attraction may be represented by a surface field

$$h_1 = [(\mu_A - \mu_B)_1 - (\mu_A - \mu_B)]/k_B T \ , \tag{1.1}$$

in which $\mu_A$ and $\mu_B$ are the chemical potentials of the two species, while the subscript 1 denotes a molecule in contact with the wall (say with its center close to $z = a$).

In the vicinity of the critical point, at $\bar{\Phi} = \Phi_c$ and $T = T_c$, the correlation length becomes large in accordance with the standard expression[2]

$$\xi(\Phi_c, T) \approx \xi_0^{\pm}/t^{\nu} \ , \tag{1.2}$$

as the temperature deviation from critical,

$$t = (T - T_c)/T_c \ , \tag{1.3}$$

becomes small. It is then reasonable to introduce a scaling hypothesis. For the case of two parallel walls at spacing

$$D = na \ , \tag{1.4}$$

and at overall critical composition ($\bar{\Phi} = \Phi_c$), most of the predictions presented in Ref. 1 follow from an extended finite-size scaling[3] postulate for the composition deviation,

$$M(z) \equiv \Phi(z) - \Phi_c \ , \tag{1.5}$$

in the asymptotic regime where $t$, $h_1 \to 0$ while $D \to \infty$. This postulate may be written

$$M(z, D; T, h_1) \approx t^{\beta} \tilde{Y}\left(\frac{z}{D}; \frac{D}{\xi}; \frac{h_1}{t^{\Delta_1}}\right) \ , \tag{1.6}$$

where we have adopted an equivalent but, as indicated by the tilde, slightly different form than used in Ref. 1. In this expression $\beta$ is the standard critical exponent[2] for the bulk coexistence curve or bulk spontaneous order, while $\Delta_1$ is a special surface exponent.[3-6] The composition, $M_1$, near the first surface may be found by setting $z = \frac{1}{2}a$ so that, as $D \to \infty$, the first argument in the scaling function $\tilde{Y}(w; x; y)$ becomes small. It then proves essential to allow for singular behavior[1,5,7] of the scaling function as $w \to 0$. Comparison with the standard finite-size scaling theory, with no $z$ dependence,[1,3,4] then yields

$$M_1(D; T, h_1) \approx t^{\beta_1} Z_0\left(\frac{D}{\xi}; \frac{h_1}{t^{\Delta_1}}\right) \ , \tag{1.7}$$

where the surface ordering exponent is given by[3-5]

$$\beta_1 = 2 - \alpha - \nu - \Delta_1 \ , \tag{1.8}$$

in which $\alpha$ is the standard specific-heat exponent.[2]

In addition, however, on the basis of a special *ad hoc* postulate[1] for the form of the free energy as a functional of the local compositon, $M(z)$, valid only for $T = T_c$, a prediction was made for the perturbations close to one wall caused by the presence of the second wall at $z = D$. For $D \to \infty$, the result may be written

$$M_1(D; T_c, h_1) - M_1(\infty; T_c, h_1) \approx A(h_1)\left(\frac{\xi_0}{D}\right)^d \ , \tag{1.9}$$

where, in general, $d$ is the *spatial dimensionality* of the system[8] (so that $d = 3$ for bulk binary fluid mixtures[1]). This expression amounts to an assertion as

 

to the form of the scaling function $Z_0$ in the limit $t \to 0$ with $Dh_1^{\nu/\Delta_1}$ large but fixed.

Although the above discussion has been presented in terms of walls placed in a near-critical binary fluid mixture, it is clear that analogous considerations apply, among other examples, to a single-component fluid near its critical point and to a binary metallic alloy which undergoes phase separation. In an ideal ferromagnet near its Curie point in zero bulk field, $M(z)$ would represent the local magnetization and $H_1 = k_B T h_1$ would be the magnetic field localized on the surface; this example, of course, has motivated the notation. However, in the different cases that may be contemplated, various extra physical effects will enter which may complicate the interpretation and experimental realizability.

It is not our purpose here to discuss such questions: rather we remark that it is certainly of interest to check the scaling postulates, (1.6) and (1.7), and the form (1.9) as far as possible theoretically. Furthermore, in order to design experiments that might effectively verify the predictions of Ref. 1 or their analogs for other systems, it would also be desirable to have quantitative estimates of the ranges in $h_1$, $t$, $D$, and $z$ over which the scaling forms should be valid, and some account of the leading corrections to the asymptotic expressions outside the scaling regions. A partial response to these needs is presented in this paper: explicitly, on the basis of previous calculations,[9,10] we discuss the analogous issues in $d = 2$ spatial dimensions using an Ising model or binary lattice gas model of the physico-chemical situation. In fact, the equivalent experimental questions can also be raised for real two-dimensional physical systems, such as monolayers adsorbed on crystalline or fluid surfaces. One may thus hope that our results will not only provide a guide to the three-dimensional case but may even be applicable more directly.

As explained in Sec. II, we find that the scaling form (1.7) is correct for a square lattice Ising model in the form of a "strip" of infinite length but of $n = D/a$ width, in which a surface field, $h_1$, is imposed on the first layer. It might be recalled that the relevant critical exponents for the $d = 2$ Ising model are

$$\alpha = 0(\log), \quad \beta = \tfrac{1}{8}, \quad \nu = 1, \quad \Delta_1 = \tfrac{1}{2}, \quad \beta_1 = \tfrac{1}{2} \quad . \tag{1.10}$$

Although it does not seem to have been pointed out explicitly in the literature before, the Pfaffian techniques[9,10] used to calculate the free energy of the $n \times \infty$ Ising strip with a surface field, $h_1$, on one boundary (the first layer), can be expected to yield explicit analytic results also for the case where a second, distinct surface field, $h_1' \equiv h_n$, is imposed on the other boundary (the $n$th layer). This is explained in the Appendix where the basic results and derived expressions for two surface fields are also presented. However, in the main text we restrict ourselves to the analytically simpler (but still quite complex) situation in which there is only one nonzero surface field Then the second or "far" wall in the model must, from the viewpoint of a binary fluid, be regarded as a neutral or nonselective wall [with $(\mu_A - \mu_B)_1 = (\mu_A - \mu_B)$]. However, this feature does not make any qualitative changes at all in the basic arguments, nor does it entail more than one or two significant quantitative changes.

Of course, it would also be valuable to check in detail the extended, spatially dependent scaling hypothesis (1.6), and this may prove feasible in future, although the necessary calculations are considerably more difficult. However, a check for $z \cong D$ is obtained in the calculations with two surface fields which are reported in the Appendix. Furthermore, our exact results for the scaling form equivalent to (1.7) (but allowing for logarithmic terms in $n$ or $t$, which arise from the logarithmic singularity of the specific heat of the two-dimensional Ising model) do precisely verify the asymptotic expression (1.9) for $M_1(D)$ as $D \to \infty$ at $T = T_c$; in fact, this result holds not just in the scaling regime. Thus the *ad hoc* free-energy functional presented in Ref. 1 may well yield exponent results which are correct in general dimensionalities. In addition, further terms in the expansion (1.9) have been derived. More generally, we obtain leading corrections to the scaling form (1.7) and, by comparison with exact numerical results, exhibit clearly the ranges over which the asymptotic behavior is achieved to desired accuracy. These results can be read off the figures presented in Sec. II; indeed, for the casual reader these figures will serve to summarize our main results. The figures display $M_1(n, T, h_1)$ in various limits, but some results for the surface susceptibility defined by[5(a)]

$$\chi_{11}(n, T, h_1) = (\partial M_1 / \partial h_1) \quad , \tag{1.11}$$

are also given explicitly and graphically.

The main technical steps in the analysis leading to the results given are explained separately in Sec. III, which utilizes the earlier calculations.[9] As mentioned, the new exact results for $n \times \infty$ strips with two distinct surface fields, $h_1$, and $h_n$, are expounded in the Appendix.

## II. SCALING RESULTS IN TWO DIMENSIONS

### A. Ising model strip of width $n$

As explained in the Introduction, we consider a plane square lattice, spin-$\frac{1}{2}$ Ising model of width $n = D/a$ rows and of infinite length. The bulk magnetic field is set equal to the critical-point value, namely zero, but a variable boundary or surface magnetic field, $H_1$, is imposed on the first row. The

basic features and general scaling properties of this model were analyzed in Ref. 9, which will be referred to as II.[10] As far as practicable, we will adhere to the notation used in II. Thus, the (positive) exchange coupling between neighboring spins is $J$, and we write

$$K = J/k_B T \quad \text{and} \quad h_1 = H_1/k_B T \ . \tag{2.1}$$

The surface magnetic field corresponds, via (1.1), to the wall specificity in the binary fluid interpretation of the model; it enters the analysis only through the variable

$$z = \tanh h_1 = h_1[1 - \tfrac{1}{3}h_1^2 + \cdots] \ . \tag{2.2}$$

(No confusion should arise with the use of $z$ as a distance coordinate in Sec. I.) The corresponding basic temperature variable is

$$t' = (1 - \sinh 2K)/(2\sinh 2K)^{1/2} \approx 2K_c t \ , \tag{2.3}$$

as $t = (T - T_c)/T_c \to 0$, with $K_c = \frac{1}{2}\ln(1+\sqrt{2}) \simeq 0.440687$.

It proves most transparent to scale by powers of $n$ in place of $t$, as done in the Introduction. Convenient scaled field and temperature variables are then[9]

$$\sigma = n^{1/2}(1+\sqrt{2})^{1/2}\tanh h_1 \sim h_1/n^{-\Delta_1/\nu} \ , \tag{2.4}$$

$$\tau = nt' \sim t/n^{-1/\nu} \ , \tag{2.5}$$

with the $d = 2$ Ising model exponents given by (1.10). However, in the limit $n \to \infty$, corresponding to a semi-infinite lattice or single wall, the scaled variable

$$\rho = \tau/\sigma^2 = t'/(1+\sqrt{2})z^2 \sim t/h_1^{1/\Delta_1} \tag{2.6}$$

is appropriate.

The local magnetization, $M(z = la) \equiv M_l$, which, via (1.5), represents the local composition imbalance in the binary fluid, is conveniently measured by the expectation value, $\langle s_l \rangle$, of an Ising spin $s_l = \pm 1$, in the $l$th lattice row. From II (2.1) to (2.7), using the relation $M_1 = n(\partial f/\partial h_1)$, in which $f$ is the reduced free energy per lattice site, we find an exact result for the surface or boundary magnetization, namely,

$$M_1(n; T, h_1) = z + z(1-z^2)\frac{2}{\pi}\int_0^1 \frac{[1 - \Lambda^{-n}(T,\omega)](1-\omega^2)^{1/2}\,d\omega}{\tilde{v}_+ + z^2(1-\omega^2) + [\tilde{v}_- - z^2(1-\omega^2)]\Lambda^{-n}(T,\omega)} \ , \tag{2.7}$$

where the $n$ dependence enters only through the factor

$$\Lambda(T,\omega) = \lambda_+/\lambda_- = [(1 + t'^2 + \omega^2)^{1/2} + (t'^2 + \omega^2)^{1/2}]^4 \ , \tag{2.8}$$

which is independent of $h_1$, while

$$\tilde{v}_\pm(T,\omega) = \frac{(1+t'^2+\omega^2)^{1/2}(t'^2+\omega^2)^{1/2} \pm [t'(1+t'^2)^{1/2}(1-\omega^2) + \tilde{c}(t)\omega^2]}{1 + \tilde{c}(t) - t'(1+t'^2)^{1/2}} \ , \tag{2.9}$$

with

$$\tilde{c}(t) = (2+t'^2)^{1/2}(1+t'^2)^{1/2} = \sqrt{2}[1 + O(t^2)] \ .$$

Our theoretical task is simply the elucidation of the analytic, scaling, and numerical properties of this formula.

### B. Semi-infinite system: critical-point behavior

When the width, $n$, of the strip increases to $\infty$ to yield a single-wall situation, the expression (2.7) simplifies since $\Lambda^{-n} \to 0$ for all $t$ and $\omega \neq 0$. Upon further specialization to the critical point, $T = T_c$ or $t' = 0$, the resulting integral can be performed exactly yielding

$$M_{1,c}^{\infty}(h_1) \equiv M_1(\infty; T_c, h_1) = \frac{z\{[1-(2+\sqrt{2})z^2]G[(1+\sqrt{2})z^2] - 1\}}{2(\sqrt{2}-1)[1-(3+2\sqrt{2})z^2]} \ , \tag{2.10}$$

where the auxiliary function is defined by

$$\tfrac{1}{4}\pi G(w) = |1 - 2\sqrt{2}w|^{-1/2}\{\ln(w^{-1}/\sqrt{2}) + \ln[1 - \sqrt{2}w + (1-2\sqrt{2}w)^{1/2}]\} \quad \text{for } w \leq \tfrac{1}{4}\sqrt{2} \ ,$$

$$= |1 - 2\sqrt{2}w|^{-1/2}\left\{\tfrac{1}{2}\pi - \tan^{-1}\frac{(1-\sqrt{2}w)}{(2\sqrt{2}w-1)^{1/2}}\right\} \quad \text{for } w \geq \tfrac{1}{4}\sqrt{2} \ . \tag{2.11}$$

Contrary to first appearances, there is no pole in $M_{1,c}^{\infty}(h_1)$ at $(3+2\sqrt{2})z^2 = 1$; likewise, the variation with $h_1$ is smooth and analytic through the point where $w = \frac{1}{4}\sqrt{2}$ or $z^2 = 1/2(2+\sqrt{2})$.

TABLE I. Coefficients for asymptotic forms. Note $B_1$, $B_2$, and $B_3$ are defined in (2.13) and $\gamma_E = 0.577\cdots$ is Euler's gamma.

| | |
|---|---|
| $B_0 = 2(1+\sqrt{2})^{1/2} K_c^{1/2} \simeq 2.06292$ | $b_0 = \frac{5}{16} B_0^2 - \frac{1}{2} - \frac{1}{4} K_c \simeq 0.7197$ |
| $b_1 = \ln(2-\sqrt{2}) - \frac{1}{4}\pi$ | $b_2 = b_1 - 2 + \sqrt{2}$ |
| $c_1 = \frac{1}{2}\ln 8 - \frac{1}{4}\pi - 1$ | $c_1^* = \frac{1}{2}\sqrt{2}$ |
| $b_1^* = \ln(8\sqrt{2}/\pi) + \gamma_E - \frac{1}{4}\pi$ | $b_3^* = b_1^* - 14(2-\sqrt{2})\zeta(3)/\pi^2$ |
| $a_3^* = 28(\sqrt{2}-1)\zeta(3)/\pi^2$ | $d_0 = \ln\frac{1}{4}\pi - \gamma_E + 7\zeta(3)/\pi^2$ |

For small fields, $h_1$, one finds the expansion

$$M_{1,c}^{\infty}(h_1) = B_1 z(\ln z^{-2} + b_1) + B_3 z^3(\ln z^{-2} + b_3) + O(z^5 \ln|z|) \ , \quad (2.12)$$

where

$$B_k = 2(1+\sqrt{2})^k/\pi \ \text{ for } k = 1, 2, 3, \ldots \ , \quad (2.13)$$

while the other coefficients are listed in Table I. Evidently, the magnetization at $T_c$ vanishes with the singular variation $h_1 \ln|h_1|$. In Fig. 1 the exact result (2.10) is plotted as a solid line. The first term in the expansion (2.12), which corresponds to the asymptotic scaling behavior (see below) is represented by the dot-dash curve: evidently, it deviates significantly from the exact result even for $h_1$ as small as 0.1. On the other hand, inclusion of the leading correction term, proportional to $z^3$, yields, as can be seen from the broken or dashed curve, reasonable accuracy up to $h \simeq 0.2$, where $M_1$ has achieved about 70% of its saturation value. Guided by this, we will exhibit the leading correction terms for nearly all the results quoted.

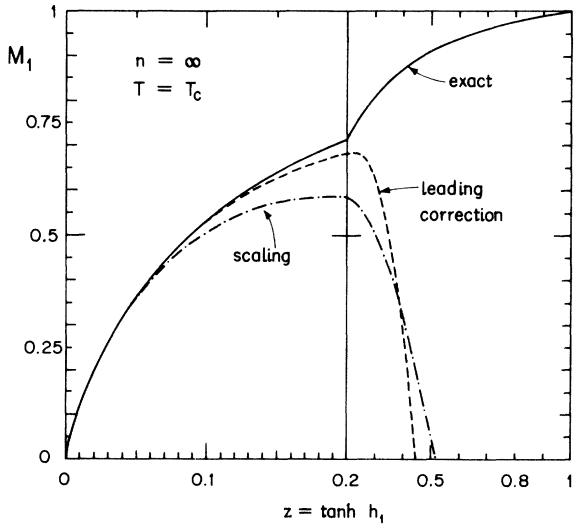


FIG. 1. Variation of the surface magnetization, $M_1$, with the reduced, surface magnetic field $h_1 \equiv H_1/k_B T$ imposed on the first row for a semi-infinite ($n = \infty$) square-lattice Ising model at its critical point. The solid curve portrays the exact result; the dot-dash curve corresponds to the leading scaling behavior containing the $h_1 \ln h_1$ singularity at low field; the broken curve incorporates the leading correction term.

### C. Semi-infinite system: scaling forms

In the critical region of the semi-infinite lattice one may hold fixed the scaling variable $\rho \sim t/h_1^2$, defined in (2.6), and study the limit $t \to 0$, or, equivalently, $z \to 0$, at fixed $\rho$.[9] This leads to the asymptotic form

$$M_1(T, h_1) = B_1 z[\ln|t'|^{-1} + \mathfrak{B}(\rho)] + B_3 z^3\{(1+\rho)[\ln|t'|^{-1} + \mathfrak{B}(\rho)] + \mathfrak{C}(\rho)\} + O(zt^2 \ln|t|) \ , \quad (2.14)$$

where $B_1$ and $B_3$ are given above, while the basic scaling function is defined by

$$\mathfrak{B}(\rho) = \tfrac{3}{2}\ln 2 - \tfrac{1}{4}\pi - (1+\rho)\mathfrak{D}(\rho) \ , \quad (2.15)$$

$$\mathfrak{D}(\rho) = \tfrac{1}{2}|1+2\rho|^{-1/2} \ln\frac{1+\rho+|1+2\rho|^{1/2}}{1+\rho-|1+2\rho|^{1/2}} \ \text{ for } \rho \geq -\tfrac{1}{2}$$
$$= |1+2\rho|^{-1/2}\cos^{-1}[-(1+\rho^{-1})] \ \text{ for } \rho \leq -\tfrac{1}{2} \ . \quad (2.16)$$

Note that the function $\mathfrak{D}(\rho)$ is smooth and analytic through $\rho = -\frac{1}{2}$ where it takes the value $\mathfrak{D}(-\frac{1}{2}) = 2$. This scaling result is quite equivalent to our previous expressions II(3.10)–(3.12), but is more transparent. The extra scaling function entering the leading correction term in (2.13) is given by

$$\mathcal{C}(\rho)=(\sqrt{2}-1)[1+(\sqrt{2}-1)(1+\rho)(1+2\rho)^{-1}][\rho^2\mathfrak{D}(\rho)-1-\rho] \ . \tag{2.17}$$

The behavior of the surface magnetization at small but fixed $h_1$ as $T\to T_c$ is determined by small $\rho$. From (2.16) one finds $\mathfrak{D}(\rho)\approx \ln 2|\rho|^{-1}$ as $\rho\to 0$, which leads back to the previous expression (2.12) for $M_{1,c}^{\infty}(h_1)$. By expanding $\mathfrak{D}(\rho)$ to higher order one obtains, for $t/h_1^2$ small,

$$M_1^{\infty}(T,h_1)-M_{1,c}^{\infty}(h_1) = D_1(z)\frac{t'}{z}+D_2(z)\frac{t'^2}{z^3}\ln|t|+O\left(\frac{t^2}{z^3}\right) \ , \tag{2.18}$$

where the coefficients $D_1$ and $D_2$ are constants for small $h_1$ (or $z$); explicitly one has

$$\tfrac{1}{2}\pi D_1(z)=1+(1+\sqrt{2})^2z^2\ln z^2 +(1+\sqrt{2})^2[\tfrac{1}{4}\pi+\sqrt{2}+\ln(1+2^{-1/2})]z^2 +O(z^4\ln|z|) \ , \tag{2.19}$$

$$\pi D_2(z)=(\sqrt{2}-1)(1-z^2) \ . \tag{2.20}$$

One sees from (2.18) that the leading temperature variation of the surface magnetization is regular, i.e., linear in $t$, whereas one might have expected an energylike, singular contribution varying as $t^{1-\alpha}\Rightarrow t\ln|t|$. However, the magnetization evidently displays a $t^{2-\alpha}\Rightarrow t^2\ln|t|$ singularity in next order.[11]

In the opposite limit, in which $h_1\to 0$ at fixed $T$, one needs the behavior of $\rho^{1/2}\mathfrak{D}(\rho)$ as $\rho\to\pm\infty$. Above $T_c$ the surface magnetization is then seen to vanish in zero field, but for $T<T_c$ one discovers a spontaneous surface magnetization

$$M_1^{\infty}(T,0+)=B_0|t|^{1/2}[1+b_0t+O(t^2)] \ , \tag{2.21}$$

where $B_0$ and $b_0$ are given in Table I.[10] Note that $\beta_1=\frac{1}{2}$, as stated in (1.10).

The quantitative nature of these results can be seen from Fig. 2 where $M_1^{\infty}$ is plotted against temperature for various small fields. As mentioned, the plots are singular, with divergent curvature at $T_c$, but this is not visible graphically. Further insight is gained by examining the surface susceptibility $\chi_{11}$, defined in (1.11). In zero magnetic field one obtains

$$\chi_{11}^{\infty}(T,0)=B_1(\ln|t'|^{-1}+c_1) +B_2t'(\ln|t'|^{-1}+c_1)+O(t^2\ln|t|) \ , \tag{2.22}$$

where the coefficient $c_1$ is included in Table I. Other explicit results, including scaling forms, may be derived straightforwardly from the expressions presented above for $M_1^{\infty}(T,h_1)$. The rounding of the susceptibility peak in a finite field can be seen from Fig. 3. Note that the maximum in $\chi_{11}^{\infty}(T)$ occurs above $T_c$ for nonzero field; again, a $t^2\ln|t|$ singularity is present at the critical point.

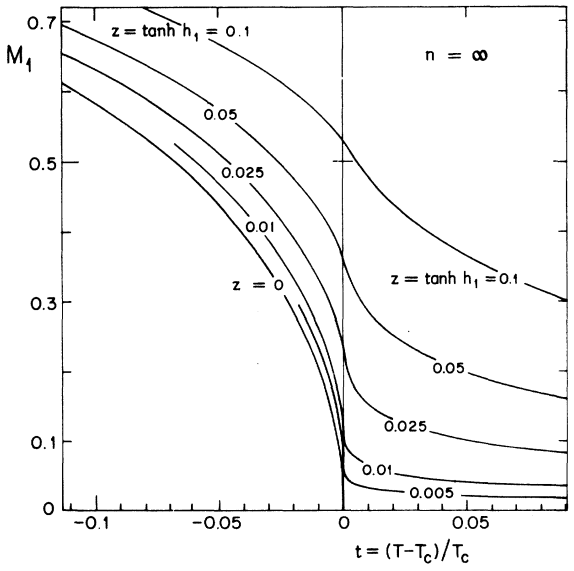


FIG. 2. Dependence of surface magnetization on temperature at small, fixed reduced surface magnetic field, $h_1\equiv H_1/k_BT$, for a semi-infinite system.

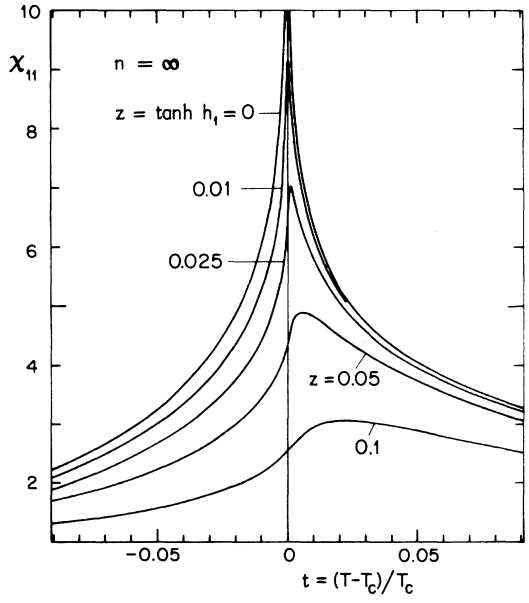


FIG. 3. Variation of the surface susceptibility, $\chi_{11}=(\partial M_1/\partial h_1)$, of a semi-infinite system at fixed reduced surface field.

### D. Finite width: scaling forms

For small values of the width $n$ the basic integral (2.7) can be evaluated exactly. This has been done for strips of width $n=1$ and 2, and the expressions found for $M_1$ have been checked against those obtained by a direct application of the transfer-matrix method. Evaluating the results at $T=T_c$ yields the curves shown in Fig. 4. More generally, the integrand can be shown to be analytic for real $\omega$ whenever $n$ is finite. Thus, as is to be anticipated, the variation of $M_1(n;T,h_1)$ is also completely smooth and analytic for $n<\infty$. In addition, then, $M_1$ always vanishes as $h_1\to 0$, and there is no spontaneous surface magnetization. On the other hand, as $n\to\infty$ below $T_c$, the initial, zero-field susceptibility, $\chi_{11}(n;T,0)$, increases exponentially fast and diverges for a semi-infinite system. This corresponds, of course, to the expected spontaneous magnetization discontinuity in the limiting magnetization isotherms below $T_c$.

It is convenient to define the finite-width contribution to the surface magnetization explicitly by writing

$$M_1(n;T,h_1)=M_1^{\infty}(T,h_1)+\Delta M_1(n;T,h_1)\ . \qquad (2.23)$$

Quite generally, one can conclude from (2.7) and (2.8) that for $T\neq T_c$ the finite-width contribution, $\Delta M_1$, decays to zero like $\exp[-4n\sinh^{-1}|t'|]$ as $n\to\infty$.[9] As we will see, however, a slower, power law decay characterizes the critical point. Furthermore, in the critical region $\Delta M_1(n;T,h_1)$ obeys a scaling law fully compatible with the result (2.14) for $M_1^{\infty}(T,h_1)$. Specifically, in terms of the scaling variable $\tau\sim nt$ and $\sigma\sim n^{1/2}h_1$, defined in (2.4) and (2.5), we obtain

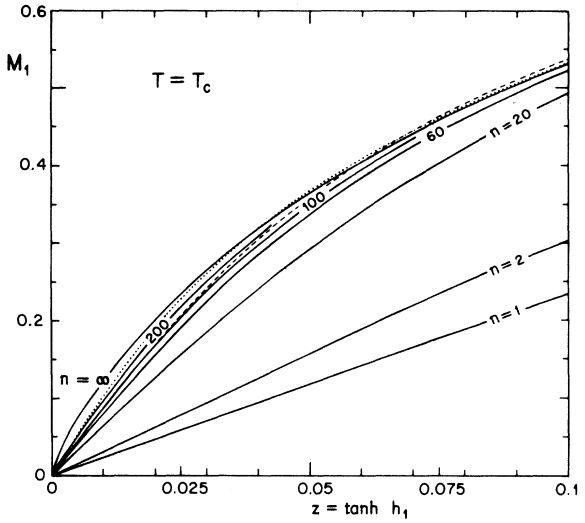


FIG. 4. Solid curves depict the variation of the surface magnetization at the critical point for systems of finite width $n=D/a$ with a surface field, $h_1$, acting only on the first row. The dotted and dashed curves represent corresponding results for strips with a surface field $h_1=h_n\equiv H_n/k_BT$ imposed on *both* first and $n$th rows for $n=60$ and $n=20$, respectively.

$$\Delta M_1=-B_1z\mathfrak{B}^*(\tau,\sigma^2)+2(z/n\pi)[(\tau+\sigma^2)\mathfrak{B}^*(\tau,\sigma^2)-\mathfrak{C}^*(\tau,\sigma^2)]+O(n^{-2}\ln n)\ , \qquad (2.24)$$

as $n\to\infty$, where $B_1$ is given by (2.13).

The scaling functions can now be represented only as integrals. Thus, writing

$$X(\xi^2)=(\tau^2+\xi^2)^{1/2}\ , \qquad (2.25)$$

we obtain

$$\mathfrak{B}^*(\tau,\sigma^2)=2\int_0^{\infty}\frac{d\xi X(\xi)e^{-4X(\xi)}/[1+e^{-4X(\xi)}]}{[X(\xi)+\tau+\sigma^2][X(\xi)+(\tau+\sigma^2)\tanh 2X(\xi)]}\ , \qquad (2.26)$$

with a similar but more complex expression for $\mathfrak{C}^*(x)$ which is presented below in (3.5).

### E. Finite width: critical-point behavior

For $T=T_c$ (or $\tau=0$) one may derive small-field expansions for the scaling functions in the form

$$\mathfrak{B}^*(0,\sigma^2)=\ln\sigma^{-2}-\sum_{m=0}^{\infty}\mathcal{G}_{m+1}(-2\sigma^2)^m\ , \qquad (2.27)$$

$$\mathfrak{C}^*(0,\sigma^2)=-(1+\tfrac{1}{2}\sqrt{2})\left[1-2\sigma^2(\ln\sigma^{-2}-1)-\sum_{l=1}^{\infty}[(l+1)\mathcal{G}_l-l\mathcal{G}_{l+1}](-2\sigma^2)^l\right]\ , \qquad (2.28)$$

where the coefficients $\mathcal{J}_l$ are linear combinations of Riemann zeta functions. The first few are listed in Table II; a general integral expression is given in (3.6). Similarly, one finds expansions valid for large $n$ (at fixed $h_1$) in the form

$$\mathfrak{B}^*(0,\sigma^2)=\sum_{l=1}^{\infty}\mathcal{J}_{l,l}(-2\sigma^2)^{-(l+1)}\ , \tag{2.29}$$

$$\mathfrak{C}^*(0,\sigma^2)=(1+\tfrac{1}{2}\sqrt{2})\sum_{l=1}^{\infty}\mathcal{J}_{l+2,l}(l+1)(-2\sigma^2)^{-(l+2)}\ , \tag{2.30}$$

where the leading coefficients are included in Table II. The general coefficient, $\mathcal{J}_{j,k}$, is discussed in Sec. III.

From these expressions we can obtain the surface magnetization at the critical point. Consider first the behavior as $h_1\to 0$ at fixed, but large $n$: one obtains the asymptotic expression

$$\begin{aligned}M_1(n;T_c,h_1)=&B_1z(\ln n+b_1^*+c_1^*n^{-1})\\&+B_3z^3(-a_3^*n+\ln n+b_3^*)\\&+O(z^5n^2,\ z^3n^{-1},\ zn^{-2}\ln n)\ ,\end{aligned} \tag{2.31}$$

where the new coefficients are given in Table I. The corresponding plots of the critical-point surface magnetization versus field are displayed in Fig. 4 for $n=20$, 60, 100, 200, and $\infty$. Evidently, the susceptibility remains finite for all finite $n$ and only the limiting curve for a semi-infinite lattice displays the divergent susceptibility $\chi_{11}\sim -\ln|h_1|$.

Finally, by utilizing (2.29) and (2.30), we can study the limit relevant to the conjecture (1.9) of Ref. 1, namely $n\to\infty$ at fixed $h_1$. We find

$$\Delta M_1(n;T_c,h_1)=-\frac{A_1^0(h_1)}{z^3n^2}\left[1-\frac{a_1^0}{z^2n}+O\left(\frac{1}{n^2z^4}\right)\right]\ , \tag{2.32}$$

where the zero superscripts serve as a reminder that the field on the far wall is $h_n\equiv 0$ (see further in the Appendix); the amplitudes are

$$\begin{aligned}A_1^0(h_1)&=\tfrac{1}{24}\pi(\sqrt{2}-1)(1-z^2)\ ,\\ a_1^0&=\sqrt{2}-1\ .\end{aligned} \tag{2.33}$$

Thus the leading critical point decay of $\Delta M_1$ for large $n$ (or $D$) is proportional to $1/n^d$ with $d=2$, in complete accord with the conjecture![1] Note that these results can also be obtained directly from the exact form (2.7) by setting $T=T_c$, subtracting the limiting form with $\Lambda^{-n}\to 0$, noting that $\Lambda^{-n}=e^{-\phi}$ with $\phi=4n\sinh^{-1}\omega$, replacing the integration variable $\omega$ by $\phi$, and expanding the integrand in inverse powers of $\sigma^2\propto z^2n$. The higher order terms in (2.32) are then seen to be of the form $a_k(z^2)/z^{2k}n^k$ where $a_k(w)$ is a polynomial of degree at most $k$. The expansion is asymptotic and there are additional correction terms of order $\exp(-8K_cn)$.

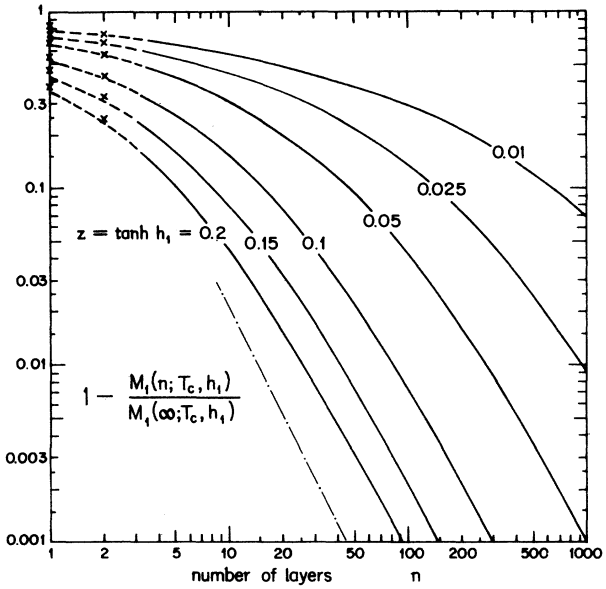


FIG. 5. Log-log plot of the relative deviation in surface magnetization $|\Delta M_1(n,T_c,h_1)/M_1^{\infty}(T_c,h_1)|$, vs the width $n=D/a$, for Ising strips at criticality under various surface fields $h_1$ imposed on the first layer. The slope of the dot-dash line is $-2$. The crosses for $n=1$ and $n=2$ represent the exact results and serve to indicate the accuracy of the scaling term plus the leading, $n^{-1}$, correction.

In Fig. 5 the relative reduction in surface magnetization, $\Delta M_1(n)/M_1(\infty)$, due to the far-wall effect has been displayed on a log-log plot using the full ex-

TABLE II. Coefficients for expanding the scaling functions $\mathfrak{B}^*(0,\sigma^2)$ and $\mathfrak{C}^*(0,\sigma^2)$.

| | | |
|---|---|---|
| $\mathcal{J}_1=\gamma_E-\ln\frac{1}{8}\pi$ | | $\mathcal{J}_2=14\zeta(3)/\pi^2$ |
| $\mathcal{J}_3=186\zeta(5)/\pi^4-7\zeta(3)/\pi^2$ | | |
| $\mathcal{J}_4=2540\zeta(7)/\pi^6-165\frac{1}{3}\zeta(5)/\pi^4$ | | |
| $\mathcal{J}_{1,1}=\pi^2/12$ | $\mathcal{J}_{2,2}=\pi^2/6$ | $\mathcal{J}_{3,3}=\frac{1}{4}\pi^2[1+(\pi^2/30)]$ |
| $\mathcal{J}_{4,4}=4\zeta(4)+2\zeta(2)$ | | $\mathcal{J}_{5,5}=3\frac{3}{4}\zeta(6)+12\frac{1}{2}\zeta(4)+2\frac{1}{2}\zeta(2)$ |
| $\mathcal{J}_{6,6}=34\frac{1}{2}\zeta(6)+30\zeta(4)+3\zeta(2)$ | | |
| $\mathcal{J}_{3,1}=\pi^4/120$ | | $\mathcal{J}_{4,2}=2\pi^4/45$ |
| $\mathcal{J}_{5,3}=3\frac{3}{4}[\zeta(6)+2\zeta(4)]$ | | $\mathcal{J}_{6,4}=30\zeta(6)+15\zeta(4)$ |

pressions (2.24), (2.29), and (2.30). Even though the basic formula is valid only for large $n$, the accuracy even at $n=1$ and $n=2$ is quite reasonable, as can be seen from the crosses which mark the exactly calculated values. For moderately large values of $h_1$, corresponding to walls strongly attractive to one species, the asymptotic $1/n^2$ decay law sets in fairly rapidly. (Note the dot-dash line of slope $-2$.) However the fractional changes in $M_1$, or in composition, in this range are only of order $10^{-2}$ to $10^{-3}$ which may be hard to detect experimentally.

### F. Finite width: critical region

For $T \neq T_c$, and hence $\tau \neq 0$, it is not hard to show that the scaling functions obey

$$\mathfrak{B}^*(\tau, \sigma^2), \quad \mathfrak{C}^*(\tau, \sigma^2) \sim (2\sigma^2\tau + \sigma^4)^{-1/2} e^{-4\tau} \ , \tag{2.34}$$

as $\tau \to \infty$ (i.e., as $n \to \infty$). This confirms the exponential decay of the finite width corrections already mentioned. For small $\tau$ and $\sigma^2$ one may expand in the form

$$\begin{aligned}\mathfrak{B}^*(\tau, \sigma^2) = &\ln|\tau|^{-1} - [1 + (\tau/\sigma^2)]\mathfrak{D}(\tau/\sigma^2) \\ &+ \ln\tfrac{1}{4}\pi - \gamma_E + 28[\zeta(3)/\pi^2](\tau + \sigma^2) \\ &+ O(\tau^2, \tau\sigma^2, \sigma^4) \ ,\end{aligned} \tag{2.35}$$

where $\mathfrak{D}(\rho)$ was defined in (2.16), with a similar expression for $\mathfrak{C}^*(\tau, \sigma^2)$ given below in (3.20). To corresponding order the scaling form for $M_1(n; T, h_1)$

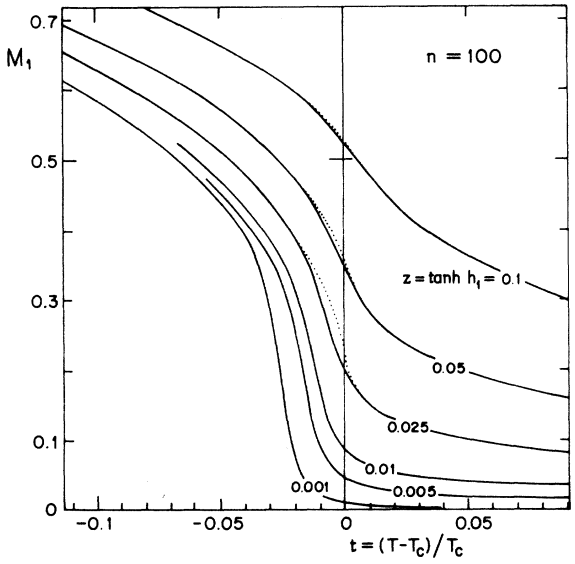


FIG. 6. Surface magnetization vs temperature for systems of width $n = D/a = 100$ in various fixed reduced surface fields $h_1$ (acting only on the first row). The dotted sections indicate the results for $n = \infty$ from Fig. 2.

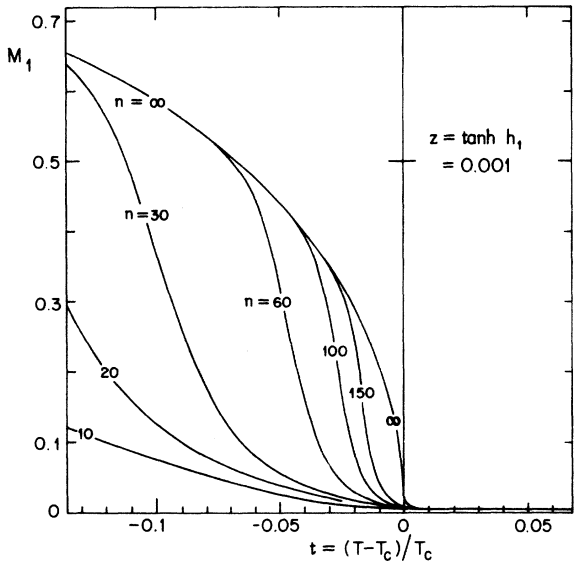


FIG. 7. Width and temperature dependence of the surface magnetization at the small fixed reduced field $\tanh h_1 = 0.001$ (with $h_n = 0$).

for small $\tau$ and $\sigma$ is obtained from (2.31) merely by replacing the factor $z^3$ by $(\sqrt{2}-1)z(\tau+\sigma^2)/n$.

To evaluate the basic expression (2.24) for general $\tau$ and $\sigma$, the most singular, logarithmic parts of the integrals defining $\mathfrak{B}^*$ and $\mathfrak{C}^*$ [in (2.26) and (3.5)] should be removed, as explained in Sec. III. The remaining integrals are tractable numerically and lead to the results shown in Figs. 6 and 7. The first figure displays the variation of the surface magnetization with temperature for a system of width $n = 100$. Although there is no spontaneous magnetization, $M_1$ becomes large below $T_c$ even in very small fields. Figure 7 shows the complementary dependence on the width $n$ in a small fixed surface field, $h_1 \simeq 0.001$: the exponential increase of the initial surface susceptibility below $T_c$ (which was mentioned above) is reflected in a strong $n$ dependence of the surface magnetization.

## III. CALCULATIONAL DETAILS

In this section we outline some of the detailed calculations leading to the results presented in Sec. II for a single surface field $h_1$, and record some of the longer explicit expressions needed for evaluating the leading corrections to scaling. (Recall that the Appendix treats the case $h_1$, $h_n \neq 0$.)

As explained, the basic formula following from I is the exact integral expression (2.7) for $M_1(n; T, h_1)$. The steps leading to the critical-point results (2.10) and (2.12) are straightforward. The scaling form (2.14) is obtained by introducing the scaling variable

$\rho \sim t/h_1^2$ and expanding in $t$ at fixed $\rho$. The results (2.18), (2.21), and (2.22) follow directly.

To analyze the situation for finite $n$ it is useful to rewrite (2.7) by introducing

$$x \equiv x(\omega) = (t'^2 + \omega^2)^{1/2} \ , \tag{3.1}$$

and using hyperbolic functions to obtain

$$M_1(n;T,h_1) = z + z(1+\tilde{c}-\tilde{d})\frac{2}{\pi}\int_0^1 \frac{\tanh[2n \sinh^{-1}x(\omega)](1-\omega^2)^{1/2}\,d\omega}{x(1+x^2)^{1/2} + [\tilde{c}\omega^2 + \tilde{d}(1-\omega^2)]\tanh(2n \sinh^{-1}x)} \ , \tag{3.2}$$

where for brevity we have written

$$\tilde{d}(t,z) = t'(1+t'^2)^{1/2} + [1+\tilde{c}-t'(1+t'^2)^{1/2}]z^2 \ , \tag{3.3}$$

while $\tilde{c}$ is defined just after (2.9). The boundary contribution for finite $n$, defined in (2.23), can then be written

$$\frac{-\pi\Delta M_1}{4z(1+\tilde{c}-\tilde{d})} = \int_0^1 \frac{d\omega\,(1-\omega^2)^{1/2}x(1+x^2)^{1/2}e^{-4ns(\omega)}/[1+e^{-4ns(\omega)}]}{[x(1+x^2)^{1/2} + \tilde{c}\omega^2 + \tilde{d}(1-\omega^2)]\{x(1+x^2)^{1/2} + [\tilde{c}\omega^2 + \tilde{d}(1-\omega^2)]\tanh 2ns(\omega)\}} \ , \tag{3.4}$$

where $s(\omega) = \sinh^{-1}x(\omega)$. The exponential decay of $\Delta M_1$ as $n \to \infty$, follows directly from this expression. Introducing the scaling variables $\tau$ and $\sigma$, holding them fixed, and allowing $n$ to become large then yields the scaling result (2.24). The leading scaling function, $\mathcal{B}^*(\tau, \sigma^2)$, is given by (2.26) which is clearly parallel to the exact result (3.4). The scaling function for the $O(1/n)$ correction term is found to be

$$\mathcal{C}^*(\tau, \sigma^2) = -2\int_0^\infty \frac{d\xi\, e^{-4X}X[(2+\sqrt{2})\xi^2 - \tau\sigma^2][X + X\tanh 2X + 2(\tau+\sigma^2)\tanh 2X]}{(1+e^{-4X})(X+\tau+\sigma^2)^2[X + (\tau+\sigma^2)\tanh 2X]^2} \ , \tag{3.5}$$

where, as in (2.25), $X \equiv X(\xi) = (\tau^2 + \xi^2)^{1/2}$.

Specializing to the critical temperature, $\tau = 0$, and expanding the factor $(\xi + \sigma^2 \tanh 2\xi)^{-1}$ in powers of $\sigma^2$ yields the series (2.27) for $\mathcal{B}^*(0, \sigma)$, with coefficient $\mathcal{I}_1$ as given in Table II, while for $k \geq 2$ one has

$$\mathcal{I}_k = \int_0^\infty (\xi^{-1}\tanh\xi)^k\,d\xi \ . \tag{3.6}$$

For given $k$, this integral can be reduced to sums of Riemann zeta functions, $\zeta(2j-1)$ with $j \leq k$, as evidenced in Table II. The complementary series, (2.29), in inverse powers of $\sigma^2$, entails the general coefficient

$$\mathcal{I}_{j,k} = \int_0^\infty \xi^j(\coth^k\xi - 1)\,d\xi \ . \tag{3.7}$$

For $k = 1$ this yields

$$\mathcal{I}_{j,1} = \Gamma(j+1)\zeta(j+1)/2^j \ , \tag{3.8}$$

while integration by parts gives the recursion relation

$$\mathcal{I}_{j,k} = \mathcal{I}_{j,k-1} + j(k-1)^{-1}\mathcal{I}_{j-1,k-1} \ , \tag{3.9}$$

from which the results quoted in Table II follow. The series expansions (2.28) and (2.30) for $\mathcal{C}^*(0, \sigma^2)$ are obtained in parallel fashion. The series in inverse powers of $\sigma^2 \propto n$ is relevant to the conjecture (1.9), concerning the far-wall effects on properties at the near wall; further scaling terms in the result (2.32) follow by using the full series.

To analyze the scaling functions for nonzero $\tau$ the scaling function $\mathcal{B}^*$ is decomposed as

$$\mathcal{B}^*(\tau, \sigma^2) = \mathcal{B}_0^* - \mathcal{B}_1^* + \mathcal{B}_2^* \ , \tag{3.10}$$

with the leading singular contribution

$$\mathcal{B}_0^* = \int_0^1 \frac{d\xi}{X(\xi)+\tau+\sigma^2} = \ln|\tau|^{-1} + \ln[1+(1+\tau^2)^{1/2}] - (1+\tau\sigma^{-2})\,\mathcal{E}(t, \sigma^2) \ , \tag{3.11}$$

for which one finds

$$\mathcal{E}(\tau, \sigma^2) = \tfrac{1}{2}|1+2\tau\sigma^{-2}|^{-1/2}\ln\left|\frac{\tau^2 + (\tau+\sigma^2)(1+\tau^2)^{1/2} + (2\tau\sigma^2+\sigma^4)^{1/2}}{\tau^2 + (\tau+\sigma^2)(1+\tau^2)^{1/2} - (2\tau\sigma^2+\sigma^4)^{1/2}}\right| \quad \text{for } -2\tau \leq \sigma^2 \ ,$$

$$= |1+2\tau\sigma^{-2}|^{-1/2}\cos^{-1}\left\{\frac{\tau^2 + (\tau+\sigma^2)(1+\tau^2)^{1/2}}{|\tau|[\tau+\sigma^2+(1+\tau^2)^{1/2}]}\right\} \quad \text{for } -2\tau \geq \sigma^2 \ , \tag{3.12}$$

while the remaining nonsingular integrals are

$$\mathfrak{B}_1^*(\tau,\sigma^2)=\int_0^1 \frac{\tanh 2X(\xi)\,d\xi}{X(\xi)+(\tau+\sigma^2)\tanh X(\xi)}\ , \quad (3.13)$$

$$\mathfrak{B}_2^*(\tau,\sigma^2)= 2\int_1^\infty \frac{d\xi\, Xe^{-4X}/(1+4e^{-4X})}{(X+\tau+\sigma^2)[X+(\tau+\sigma^2)\tanh 2X]}\ . \quad (3.14)$$

When $\tau$ and $\sigma^2$ are small one finds

$$\mathcal{S}(\tau,\sigma^2)=\mathfrak{D}(\tau/\sigma^2)-\sigma^2+O(\tau^2,\tau\sigma^2,\sigma^4)\ , \quad (3.15)$$

$\mathfrak{D}$ being defined in (2.16), while $\mathfrak{B}_1^*$ and $\mathfrak{B}_2^*$ may be expanded straightforwardly in powers of $\tau$ and $\sigma^2$. This yields the expression (2.35).

The correction scaling function for $\tau$ nonzero can be decomposed similarly as

$$\mathcal{C}^*(\tau,\sigma^2)=-\mathcal{C}_0^*+\mathcal{C}_1^*-\mathcal{C}_2^*\ , \quad (3.16)$$

with

$$\mathcal{C}_0^*=\int_0^1 C_0(\xi;\tau,\sigma^2)\,d\xi \equiv \int_0^1 \frac{[(2+\sqrt{2})\xi^2-\tau\sigma^2]\,d\xi}{[X(\xi)+\tau+\sigma^2]^2}\ , \quad (3.17)$$

$$\mathcal{C}_1^*=\int_0^1 C_1(\xi;\tau,\sigma^2)\,d\xi \equiv \int_0^1 \frac{[(2+\sqrt{2})\xi^2-\tau\sigma^2]\tanh^2 2X(\xi)\,d\xi}{[X(\xi)+(\tau+\sigma^2)\tanh 2X(\xi)]^2}\ , \quad (3.18)$$

$$\mathcal{C}_2^*=\int_1^\infty [C_0(\xi;\tau,\sigma^2)-C_1(\xi;\tau,\sigma^2)]\,d\xi\ , \quad (3.19)$$

in which the integrands $C_0(\xi)$ and $C_1(\xi)$ are defined in the obvious way. The first integral can again be computed exactly; the other two can be expanded in powers of $\tau$ and $\sigma^2$ or, for graphical purposes, calculated by numerical integration. In this way one finds

$$\mathcal{C}^*(\tau,\sigma^2)=-(1+\tfrac{1}{2}\sqrt{2})+2(2+\sqrt{2})(\tau+\sigma^2)[\ln|\tau|^{-1}-(1+\tau\sigma^{-2})\mathfrak{D}(\tau/\sigma^2)+d_0] -[2+\sqrt{2}-\tau(2\tau+\sigma^2)^{-1}][\tau+\sigma^2-\tau^2\sigma^{-2}\mathfrak{D}(\tau/\sigma^2)]+O(\tau^2,\tau\sigma^2,\sigma^4)\ , \quad (3.20)$$

where $d_0$ is in Table II. In comparing with (2.15) to (2.17) for the scaling function $\mathcal{B}(\rho)$ and $\mathcal{C}(\rho)$, one finds that the various singular terms in $\tau$ and $\sigma$ cancel and one obtains a scaling expansion for $M_1(n;T,h_1)$ in powers of $\tau$ and $\sigma^2$ valid for large but finite $n$.

*Note added in proof.* Attention should be drawn to recent work by R. Z. Bariev [Theor. Math. Phys. (USSR) 40 (1979)] on the local magnetization of the semi-infinite Ising model and by D. B. Abraham [private communication and unpublished] which also addresses the problem of a lattice of finite width with surface fields on both boundaries. These analyses provide further checks on the phenomenological scaling postulates (1.6) and (A27) following from Ref. 1.

## ACKNOWLEDGMENTS

We are indebted to Professor P.-G. de Gennes for discussions which stimulated this work. Support has been provided by the National Science Foundation, in part through the Materials Science Center at Cornell University. An award from the John Simon Guggenheim Memorial Foundation is gratefully acknowledged by M.E.F.

## APPENDIX: ISING STRIP WITH TWO SURFACE FIELDS

Calculations to study the Ising model with finite dimensions have, for the most part, been based on the Pfaffian-dimer method which yields an expression for the partition function of any finite *planar* Ising model in zero magnetic field as the square root of a finite antisymmetric determinant.[10,12] To construct the partition function of a finite Ising strip of $n$ layers or rows of spins each of length $m$ spins, with nearest-neighbor interactions and a reduced surface field, $h_1$, imposed on all the spins in the first layer and a distinct surface field, $h_n \equiv h_1'$, imposed on all spins in the last or $n$th layer, we may proceed as follows. Consider a *cylinder* of length $ma$ and circumference $(n+1)a$ the spins being arranged at spacing $a$ in $(n+1)$ axial rows labeled $0, 1, 2, \ldots, (n-1), n$. This cylinder is, of course, equivalent to a strip of $(n+1)$ rows with periodic boundary conditions across the strip.

Now an Ising model of spins $s_{\vec{r}}$, $s_{\vec{r}'}$, ... connected by pairwise interactions $J(\vec{r};\vec{r}')s_{\vec{r}}s_{\vec{r}'}$ can be represented by a linear graph, $\mathcal{G}$, in which each spin $s_{\vec{r}}$ corresponds to a vertex labeled $\vec{r}$ of $\mathcal{G}$, and each nonzero interaction $J(\vec{r},\vec{r}')$, corresponds to a bond or edge $(\vec{r},\vec{r}')$ of $\mathcal{G}$.[13] Planarity of the Ising model

means that the associated graph $\mathcal{G}$ can be embedded in the plane with no crossing bonds.[13] The graph representing the cylinder of length $ma$ and circumference $(n+1)a$ is, in fact, planar as can be seen by taking polar coordinates $(r,\theta)$ in the plane and associating the $k$th spin in the $l$th row, say $s_{k,l}$, with the point

$$r_{k,l}=k, \quad \theta_{k,l}=2l\pi/(n+1) \ , \tag{A1}$$

for $k=1,2,\ldots,m$ and $l=0,1,2,\ldots,n$.

To represent the pairwise spin couplings in the original $m\times n$ Ising strip, we take the nearest-neighbor bond parameters as $J(k,l;k+1,l)=J_1$ and $J(k,l;k,l+1)=J_2$ for $k=1,2,\ldots,(m-1)$ and $l=1,2,\ldots,(n-1)$. This looks after the couplings of all spins except those in the row $l=0$; at this point we thus have an $m\times n$ strip with free-boundary conditions (and $m$ extra uncoupled spins). Finally, to represent the surface magnetic fields, we first introduce a coupling $J_0$ between all neighboring spins in the row $l=0$; i.e., we set

$$J(k,0;k+1,0)=J_0 \ , \tag{A2}$$

for $k=1,2,\ldots,(m-1)$. We will let $J_0\to\infty$, so that $\tanh(J_0/k_BT)\to 1$; this ensures that all the spins $s_{k,0}$ are frozen "up" (or, equivalently, "down"). Then the surface magnetic fields are introduced by coupling the $l=0$ spins to those in the first and $n$th rows by setting

$$\begin{aligned} J(k,0;k,1)&=H_1=k_BTh_1 \ , \\ J(k,0;k,n)&=H_n=k_BTh_n \ , \end{aligned} \tag{A3}$$

for $k=1,2,\ldots,m$. Since the spins $s_{k,0}$ all take the value $+1$ (or all $-1$), this introduces the correct Boltzmann factors $\exp(h_1 s_{k,1})$ and $\exp(h_n s_{k,n})$ into the partition function. The effect of the second option ($s_{k,0}=-1$, all $k$) is merely that the partition function calculated for the cylinder will be *twice* the desired partition function for the strip with surface magnetic fields.

The partition function can now be expressed in terms of a single determinant which can be evaluated asymptotically in compact form in the limit $m\to\infty$ by established methods.[10,12] An alternative procedure, which will lead to the identical final result, is to consider an $m\times(n+1)$ torus with a similar special row of spins with couplings $J_0\to\infty$, $k_BTh_1$, and $k_BTh_n$. Although a torus does not yield a planar graph it is possible to express its partition function, $Z_{mn}$, exactly in terms of the square roots of four, slightly different antisymmetric determinants as expounded by McCoy and Wu.[10(b)] It proves convenient to take $m$ even (which clearly makes no difference in the limit $m\to\infty$) and in both the analysis of the torus and the cylinder one needs $n\geq 2$. The required determinants are found to be equal in pairs but care is needed in determining the appropriate signs for their square roots. The issue is most readily decided by considering the limit $J_1\to 0$, in which case the system decomposes into $m$ independent one-dimensional chains (or "rings") each of which has a partition function including the crucial factor $(1+zz'z_2^{n-1})$ where we have adopted the notation

$$z=\tanh h_1, \quad z'=\tanh h_n, \quad z_i=\tanh K_i \ , \tag{A4}$$

for $i=1,2$ with

$$K_1=J_1/k_BT, \quad K_2=J_2/k_BT \ . \tag{A5}$$

One discovers that the condition

$$zz'z_2^{n-1}\geq 0 \quad (n\geq 2) \ , \tag{A6}$$

leads to all positive signs, so that the partition function is given as the sum of the square roots of two determinants which asymptotically, as $m\to\infty$, become effectively equal. (The converse case, $zz'z_2^{n-1}<0$ leads to a difference of almost equal determinants which is much harder to analyze: however, as explained below, this difficulty can be sidestepped.)

Evaluation of the logarithm of the determinants involved leads, as usual to integrals. The final result for the free energy per spin of the $n\times\infty$ lattice with two distinct surface fields may be written, subject to (A6), as

$$\begin{aligned} f(n,t;h_1,h_n)&=-F/k_BT=\lim_{m\to\infty}(mn)^{-1}\ln Z_{mn} \\ &=\ln(2\cosh K_1\cosh K_2)+n^{-1}\ln(\cosh h_1\cosh h_n/\cosh K_2) \\ &\quad+n^{-1}\int_0^{2\pi}\frac{d\theta}{4\pi}\ln\{|1+z_1e^{i\theta}|^{2n}[p_+(z)p_+(z')\lambda_+^n+p_-(z)p_-(z')\lambda_-^n]\} \ , \end{aligned} \tag{A7}$$

where, with

$$a=\frac{2iz_1\sin\theta}{|1+z_1e^{i\theta}|^2}, \quad b=\frac{1-z_1^2}{|1+z_1e^{i\theta}|^2}, \quad c=\frac{2i\sin\theta}{|1+e^{i\theta}|^2} \ , \tag{A8}$$

one has $\lambda_+\geq\lambda_-$ and, explicitly

$$\lambda_\pm(\theta;z_1,z_2)=\tfrac{1}{2}(z_2^2-a^2+b^2)\pm\tfrac{1}{2}\Delta(\theta;z_1,z_2) \ , \tag{A9}$$

$$\Delta^2=(b^2-a^2-z_2^2)^2-4a^2z_2^2 \ , \tag{A10}$$

with square root chosen so that $\Delta = b^2 - a^2 \geq 0$ when $z_2 \to 0$. Lastly, with

$$v(\theta;z_1,z_2) = \frac{1}{\sqrt{2}}\left[1 + \frac{b^2 - a^2 - z_2^2}{\Delta}\right]^{1/2} ,$$

$$\bar{v}(\theta;z_1,z_2) = \frac{-1}{\sqrt{2}}\left[1 - \frac{b^2 - a^2 - z_2^2}{\Delta}\right]^{1/2} , \quad \text{(A11)}$$

so that $v^2 + \bar{v}^2 = 1$, one has

$$p_+(\theta;z_1,z_2;z) = v - i\bar{v}z^2/cz_2 , \quad \text{(A12)}$$

$$p_-(\theta;z_1,z_2;z) = \bar{v} + ivz^2/cz_2 . \quad \text{(A13)}$$

One may now check that when $z_1 \to 0$ the expression (A7) yields the correct free energy for a single chain of $n$ spins with fields $h_1$ and $h_n$ acting on first and last spins. Likewise if $z_2 \to 0$ one obtains the free energy corresponding to $(n-2)$ infinite Ising chains in zero field plus two infinite chains, one in a field $h_1$ and one in a field $h_n$. Finally in the case $n = 2$ one checks, after much algebra,[14] that the free energy given for a two-layer strip with fields $h_1$ and $h_2$ acting on the first and second layers is the same as that calculated by diagonalizing the appropriate $4 \times 4$ transfer matrix.[15]

For further examination of this result we specialize to the case $J_1 = J_2$ or $z_1 = z_2$. Then we may rewrite the result (A7) in the convenient form

$$f(n;T,h_1,h_n) = f_\infty(T) + n^{-1}[f^\times(T,h_1) + f^\times(T,h_n)] + n^{-1}f^*(n;T,h_1,h_n) , \quad \text{(A14)}$$

where the usual bulk free energy, first found by Onsager,[10] can be expressed as

$$f_\infty(T) = \tfrac{1}{2}\ln 2\sinh 2K + \pi^{-1}\int_0^1 d\omega\,(1-\omega^2)^{-1/2}\ln\lambda_+(T,\omega) , \quad \text{(A15)}$$

while the surface contribution for a semi-infinite lattice is[1,10]

$$f^\times(T,h_1) = \ln\cosh h_1 - \tfrac{1}{2}\ln\cosh K - \tfrac{1}{4}\ln 2 + \pi^{-1}\int_0^1 d\omega(1-\omega^2)^{-1/2}\ln[v_+^{-1/2}(v_+ + z^2u)] . \quad \text{(A16)}$$

Finally, the finite-size interference term for two fields is

$$f^*(n;T,h_1,h_n) = \frac{1}{\pi}\int_0^1 \frac{d\omega}{(1-\omega^2)^{1/2}}\ln\left[1 + \Lambda^{-n}\frac{v_+(v_- - z^2u)(v_- - z'^2u)}{v_-(v_+ + z^2u)(v_+ + z'^2u)}\right] . \quad \text{(A17)}$$

In these expressions we may now write

$$\lambda_\pm(T,\omega) = 1 + 2t'^2 + 2\omega^2 \pm (t'^2 + \omega^2)^{1/2}(1 + t'^2 + \omega^2)^{1/2} , \quad \text{(A18)}$$

while $\Lambda(T,\omega) = \lambda_+/\lambda_-$ was defined also in (2.8). In addition we have

$$v_\pm(T,\omega) = \tilde{v}_\pm(T,\omega)u(T,\omega)/(1-\omega^2) , \quad \text{(A19)}$$

where $\tilde{v}_\pm(T,\omega)$ and $\tilde{c}(T)$ were defined in (2.9), and

$$u(T,\omega) = [1 + \tilde{c} - t'(1+t'^2)^{1/2}](1-\omega^2)/(t'^2+\omega^2)^{1/2}(1+t'^2+\omega^2)^{1/2} . \quad \text{(A20)}$$

Note that (A7) is symmetric in $z$ and $z'$ and reduces to previous results[1,10] if either $z$ or $z'$ vanish. By differentiating with respect to $h_1$, the surface magnetization of the first layer may be found as

$$M_1(n;t,h_1,h_n) = z + z(1-z^2)\frac{2}{\pi}\int_0^1 \frac{d\omega}{(1-\omega^2)^{1/2}}\frac{u(1-\Lambda^{-n}) + z'^2u^2(v_+^{-1} + v_-^{-1}\Lambda^{-n})}{Q_+(z,z') + \Lambda^{-n}Q_-(z,z')} , \quad \text{(A21)}$$

where the denominator terms are

$$Q_\pm(z,z';T,\omega) = (v_\pm \pm z^2u)(v_\pm \pm z'^2u)/v_\pm , \quad \text{(A22)}$$

so that (A12) reduces to (2.7) when $z' = 0$.

This result for $M_1$ simplifies appreciably if the field $h_1$ on the first layer vanishes: the integral can then be performed and one obtains

$$M_1(n;T,0,h_n) = \frac{\tilde{c}_+ z'[|\tilde{t}| - \tilde{t}\tanh(2n\sinh^{-1}|t'|)]^{1/2}}{\tilde{c}_-[|\tilde{t}| + (\tilde{t} + \tilde{c}_+z'^2)\tanh(2n\sinh^{-1}|t'|)]^{1/2}} , \quad \text{(A23)}$$

where, since $z=0$, the condition (A6) now has no force, and where for brevity we have put

$$\tilde{t}=t'(1+t'^2)^{1/2}\approx t' \ , \tag{A24}$$

$$\tilde{c}_{\pm}(T)=(2+t'^2)^{1/2}(1+t'^2)^{1/2}-\tilde{t}\pm 1\approx\sqrt{2}\pm 1 \ . \tag{A25}$$

When $t,h_n\to 0$ and $n\to\infty$, it is easy to see that this has the scaling form

$$M_1(D;T,0,h_n)\approx t^{\beta_1}Z_1\left(\frac{D}{\xi};\frac{h_n}{t^{\Delta_1}}\right) \ , \tag{A26}$$

which parallels (1.7) and corresponds to the natural expectation that both surface fields scale as $t^{\Delta_1}$ (with, in this case, $\Delta_1=\frac{1}{2}$) and yield the same surface magnetization prefactor $t^{\beta_1}$. By noting the symmetry under $M_1\Rightarrow M_n$, $h_n\Rightarrow h_1$, we see that this result also tests the $z$-dependent postulate (1.6) in the more general form

$$M(z,D;T,h_1,h_n)\approx t^{\beta}\tilde{Y}\left(\frac{z}{D};\frac{D}{\xi};\frac{h_1}{t^{\Delta_1}},\frac{h_n}{t^{\Delta_1}}\right) \ . \tag{A27}$$

However, for $w\to 0$ and $w\to 1$ the scaling function must exhibit the singular behavior[16]

$$\tilde{Y}(w;x;y,y')=w^{\theta}(1-w)^{\theta}\bar{Y}(w;x;y,y') \ , \tag{A28}$$

where $\bar{Y}(0;x;y,y')=\bar{Y}(1;x;y',y)$ is finite and nonzero, and $\theta=(\beta_1-\beta)/\nu$ (which yields $\theta=\frac{3}{8}$ in the present case).

At the critical point, $T=T_c$, further simplification ensues and one finds simply

$$M_{1,c}(n;h_n)=\frac{(1+\sqrt{2})z'}{[1+2(1+\sqrt{2})nz'^2]^{1/2}} \ . \tag{A29}$$

Thus for large $n$ the magnetization at a free wall (with zero surface field) decreases as $C/n^{1/2}$ where $C$ is *independent* of the field at the far wall, provided only this does not vanish! This decay law is in accord with the scaling prediction $1/D^{\beta_1/\nu}$ which follows from the scaling form (A26), provided the independence of the field $h_n$ at the far wall is assumed: however, this independence is not obvious *a priori!* The critical-point variation of $M_1$ following from (A29) and some similar corresponding plots for $t=-0.05$ are presented in Fig. 8.

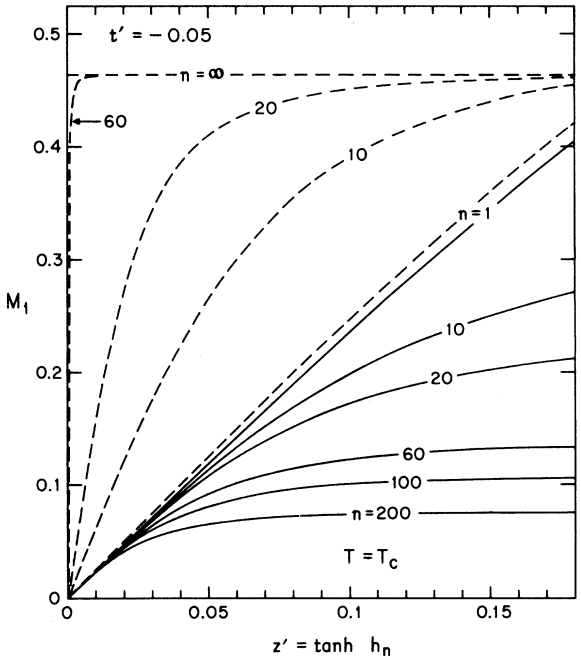


FIG. 8. Variation of the magnetization, $M_1$, of the first layer when a surface field $h_n=H_n/k_BT$ is applied only on the far boundary, i.e., on the $n$th layer with $h_1\equiv 0$: solid curves for $T=T_c$; broken curves for $t'=2K_c(T-T_c)/T_c=-0.05$.

Further results can, of course, be derived from (A21): in particular the critical-point scaling form for the difference

$$M_1(n;T,h_1,h_n)-M_1^{\infty}(T,h_1)=\Delta M_1(n;T,h_1,h_n) \ , \tag{A30}$$

[which is to be compared with (2.23)], is found to be

$$\Delta M_{1,c}(n;h_1,h_n)\approx -B_1 z[(1-z^2)\mathfrak{B}_c^*(\sigma^2,\sigma'^2)+n^{-1}\mathfrak{C}_c^*(\sigma^2,\sigma'^2)] \ , \tag{A31}$$

where $B_1$ is defined in (2.13) and, in accord with (2.4),

$$\sigma'^2=(1+\sqrt{2})n\tanh^2 h_n \ . \tag{A32}$$

The scaling function is given by

$$\mathfrak{B}_c^*(\sigma^2,\sigma'^2)=\int_0^{\infty}d\xi\left[-\frac{\sigma'^2+\xi\tanh 2\xi}{\xi^2+\sigma^2\sigma'^2+(\sigma^2+\sigma'^2)\xi\tanh 2\xi}+\frac{1}{\xi+\sigma^2}\right] \ , \tag{A33}$$

with a similar integral expression for $\mathfrak{C}_c^*(\sigma^2,\sigma'^2)$.

We have also evaluated numerically the integral involved in (A21) at the critical point, $T=T_c$, for the special case, $h_1=h_n$ of identical walls. Some of the results are included in Fig. 4 (for $n=60$: dotted curve; for $n=20$: dashed curve). As is to be expected, the surface magnetization for $h_n=h_1>0$ is always greater than that for

$h_n = 0$ at the same value of $h_1$ and $n$. More surprising, perhaps, is that the plots for $h_1 = h_n$ actually cross and rise above the magnetization curve $M_{1,c}^{\infty}(h_1)$, for the semi-infinite lattice. Likewise, for example, $M_{1,c}(n=20)$ is greater than $M_{1,c}(n=60)$ for $z = z' > 0.075$, which exceeds $M_{1,c}(n=100)$ for $z = z' > 0.049$, which in turn exceeds $M_{1,c}(n=200)$ for $z > 0.037$. This interplay of the opposing effects of a positive far-wall field and of increasing wall separation could lead to awkward experimental problems in determining the true asymptotic-decay laws.

We may also, by using the definition (A30) and the exact expression (A21), study the influence of one wall on the other as $n \to \infty$ in order to test further the conjecture (1.9). As in the derivation of the results (2.32) and (2.33) for $h_n = 0$, we proceed by setting $T = T_c$, subtracting off the limiting form with $\Lambda^{-n} \to 0$, putting $\phi = 4n \sinh^{-1}\omega$, and expanding the integrand in inverse powers of $\sigma^2 \propto nz^2$. It proves essential to assume that $h_n$ is *strictly* positive (for $z_2 > 0$). We then find

$$\Delta M_1(n; T_c, h_1, h_n) = \frac{A_1^+(h_1)}{z^3 n^2}\left[1 - \frac{a_1^+(h_1,h_n)}{z^2 n} + O\left(\frac{1}{n^2 z^4}\right)\right] , \tag{A34}$$

where the superscripts + denote the condition $h_n > 0$. As before the conjecture (1.9) is confirmed in that the perturbation in the surface magnetization decays with separation of the walls as $1/D^d$ (with, here, $d = 2$). The values of the amplitudes are

$$A_1^+(h_1) = \tfrac{1}{48}\pi(\sqrt{2}-1)(1-z^2) = -\tfrac{1}{2}A_1^0(h_1) , \tag{A35}$$

where $A_1^0(h_1)$ is the amplitude for $h_n \equiv 0$ given in (2.33), while

$$a_1^+(h_1,h_n) = (\sqrt{2}-1)[(z/z')^2 + 1 - (2+\sqrt{2})z^2] . \tag{A36}$$

A striking feature of these results is that the leading decay amplitude, say $A_1(h_1,h_n)$, is actually *independent* of the field, $h_n$, on the far wall although it clearly depends on the sign of $h_n$ and, as seen explicitly in (A35), also assumes a distinct value when $h_n$ vanishes. This general conclusion actually follows from the ansatz for the critical-point variation of the local magnetization introduced in Ref. 1.[17] However, we currently have no alternative understanding of the simple factor $-\frac{1}{2}$ relating $A_1^+(h_1)$ and $A_1^0(h_1)$. Note that the amplitude, $a_1^+$, of the leading correction term now has a significant dependence on both $h_1$ *and* $h_n$ and, indeed, diverges as $h_n \to 0$.

Finally, let us reconsider the signficance of the restriction (A6) which, for the ferromagnetic case, $J_2 > 0$, reduces simply to $h_1 h_n \geq 0$. Now the expressions (A7) and (A17) for the total free energy are invariant under the joint inversion $h_1, h_n \Rightarrow -h_1, -h_n$, which is just what is required by the symmetry of the original Hamiltonian. On the other hand, these expressions are also invariant under the *separate* inversions $h_1 \Rightarrow -h_1$ *or* $h_n \Rightarrow -h_n$: unless one of the fields vanish (or $J_2 = 0$), this cannot be correct! However no error is involved since such separate inversions clearly violate the restriction $h_1 h_n \geq 0$ and are thus disallowed. Nevertheless one concludes, at first glance, that the analysis is deficient since the free energy has been found only for fields in the first and third quadrants of the $(h_1,h_n)$ or $(z,z')$ planes. The deficiency is more apparent than real, however, since for all finite $n$ the free energy and all its derivatives are necessarily analytic functions jointly in $z$ and $z'$ (and, for that matter, in $z_1$ and $z_2$ also). Thus by analytic continuation, the free energy, the surface magnetizations, etc., may be obtained in the second and fourth quadrants of the $(h_1,h_n)$ and $(z,z')$ planes. Indeed, in writing (A23) with a prefactor $z'$ (instead of $|z'|$ which is what the analysis strictly yields in the limit $z \to 0+$) such an analytic continuation has been explicitly performed. Unfortunately it is not clear how to effect the continuation so explicitly when both fields are nonzero.

The antisymmetric case, $h_n = -h_1$, does, however, yield somewhat to further argument.[17] By reflection symmetry of one side of the $n \times \infty$ strip into the opposite side, one sees that the local magnetization must vanish at the midpoint of the strip. Asymptotically, as $D = na \to \infty$, this means that the situation $h_n = -h_1$ is equivalent to the case $h_{n'} = 0$ where the zero far-wall field is now imposed on a strip of, asymptotically, exactly, half the original width, i.e., $D' = n'a \approx \frac{1}{2}D$. This yields an amplitude which satisfies the relation[17]

$$A_1(h_1,-h_1) = -A_1^-(h_1) = -2^2 A_1^0(h_1) , \tag{A37}$$

which should, in fact, be valid for all fixed $h_n < 0$ as $n \to \infty$. More generally, in a $d$-dimensional system,[17] the factor $2^2$ should be replaced by[8] $2^d$.

[1]M. E. Fisher and P.-G. de Gennes, C.R. Acad. Sci. 287, 207 (1978).

[2]See, e.g., M. E. Fisher, Rep. Prog. Phys. 30, 615 (1967); or H. E. Stanley, *Introduction to Phase Transitions and Critical Phenomena* (Oxford University Press, New York, 1971).

[3]M. E. Fisher, in *Proceedings of the 51st Enrico Fermi Summer School, Varenna, Italy, 1970,* edited by M. S. Green (Academic, New York, 1971).

[4]M. E. Fisher, J. Vac. Sci. Tech. 10, 665 (1973).

[5]See also (a) K. Binder and P. C. Hohenberg, Phys. Rev. B 6, 3461 (1972); and (b) M. N. Barber, Phys. Rev. B 8, 407 (1973).

[6]Note that M. A. Moore and A. J. Bray, Phys. Rev. Lett. 38, 1046 (1977), have argued that one should always have $\Delta_1 = \frac{1}{2}(1-\alpha)$.

[7]Explicitly one must have $\tilde{Y}(w;x;y) \approx w^{\theta} Y_0(x,y)$ as $w \to 0$, with $\theta = (\beta_1 - \beta)/\nu$.

[8]Actually the exponent found is $(2-\alpha)/\nu$ which is equal to the dimensionality, $d$, only if the validity of *hyperscaling* is granted, see, e.g., M. E. Fisher, Proc. Nobel Symp. 24, 16 (1973).

[9]H. Au-Yang and M. E. Fisher, Phys. Rev. B 11, 3469 (1975): to be referred to as II.

[10]See also B. M. McCoy and T. T. Wu (a) Phys. Rev. 162, 436 (1967) and (b) *The Two-Dimensional Ising Model* (Harvard University Press, Cambridge, Mass., 1973), Chap. 6.

[11]The coefficient of this singularity is given erroneously in Eq. (5.39) of Ref. 10(b) owing to a misprint or slip.

[12]M. E. Fisher, J. Math. Phys. 7, 1776 (1966).

[13]For graph theoretical terminology, see e.g., J. W. Essam and M. E. Fisher, Rev. Mod. Phys. 42, 271 (1970).

[14]Because of the difficulty of carrying this check through, a few words about what is involved are in order. First, the $4 \times 4$ transfer matrix leads, for general fields, to an expression for the free energy per spin as the logarithm of the largest root, $x_1$, of a *quartic* equation. However, by methods known through the theory of equations, the roots, $x_i$, of the quartic can be related to the roots, $y_j$, of a particular *cubic* equation of the form $y^3 - I_1 y + I_0 = 0$ where $I_1$ and $I_0$ are functions of $h_1$, $h_2$, $z_1$, and $z_2$. Thence $x_1$ can be expressed as a complicated but symmetric function of the cubic roots, $y_i$. On the other hand, the general expression (A7) reduces for $n = 2$ to the integral on $\theta$ of an expression $\ln D(\theta)$ where $D(\theta)$ is found to be a cubic polynomial in $\cos\theta$. A substitution $\cos\theta = y - a$ reduces this to the *same* polynomial arising in the analysis of the transfer matrix. Factorization of $D(\theta)$ in terms of the cubic roots, $y_i$, allows the logarithmic integrals to be performed and, finally, the same expression is obtained as in the matrix approach.

[15]Another check, which is fairly stringent, is to let $z'$ (or, equivalently, $z$) take the value unity; the surface magnetic field $H_n$ then becomes infinite so the adjacent, $(n-1)$th, row of spins becomes frozen all "up". In effect this must simply reduce the width of the lattice by one row while replacing the surface magnetic field by the new value $H_{n-1} = J_2$, which derives from the bond variable $z_2$ linking spins in the $n$th and $(n-1)$th rows. The identity $\lambda_{\pm} p_{\pm}(\theta;z_1,z_2;1) = p_{\pm}(\theta;z_1,z_2;z_2)(1+z_1^2)/|1+z_1 e^{i\theta}|^2$ then ensures that the expression (A7) correctly reproduces this reduction.

[16]Compare with the derivation of (1.7) and Ref. 7.

[17]M. E. Fisher and H. Au-Yang, Physica (Utrecht) (in press).